

SUPPLEMENTARY INFORMATION

Enhanced Charge Separation in g-C₃N₄ – BiOI Heterostructures for Visible Light Driven Photoelectrochemical Water Splitting

Kazi Alam,^{1†} Pawan Kumar,^{1†} Piyush Kar,¹ Ujwal Thakur,¹ Sheng Zeng,¹ Kai Cui² and Karthik Shankar¹

¹Department of Electrical & Computer Engineering, University of Alberta, Edmonton, AB T6G 1H9 Canada

²Nanotechnology Research Centre, National Research Council of Canada, Edmonton, Canada T6G 2M9

*corresponding author's email address: kshankar@ualberta.ca

†These authors contributed equally

Applied bias photon-to-current efficiency (ABPE):

The ABPE% was calculated by using following formula:

$$\text{ABPE (\%)} = [J (\text{mA cm}^{-2}) \times (1.23 - V_b) / P (\text{mW cm}^{-2})] \times 100 \dots\dots\dots \text{Eqn- (1)}$$

Where, J is the current density, V_b is applied voltage at RHE scale and P is power density of the incident light.

The applied voltage on Ag/AgCl scale was converted RHE scale by using following expression.

$$V_{\text{RHE}} = V_{\text{Ag/AgCl}} + 0.059 \text{ pH} + V^0_{\text{Ag/AgCl}} \dots\dots\dots \text{Eqn - (2)}$$

Where; $V^0_{\text{Ag/AgCl}} = 0.197 \text{ V}$.

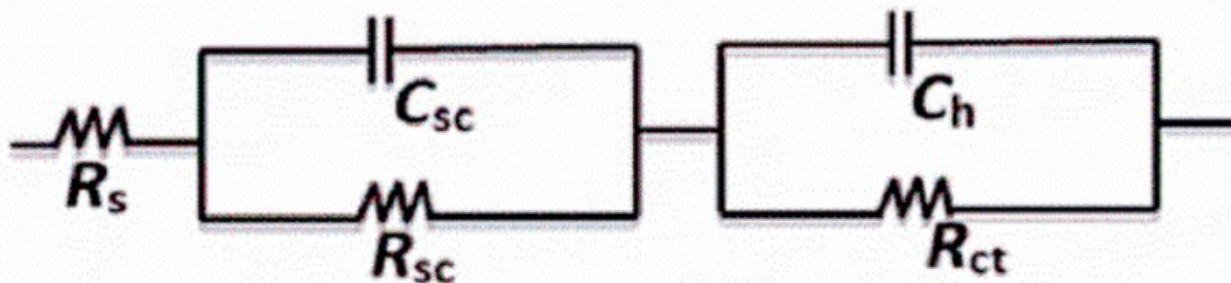


Figure S1. Equivalent circuit used to model the EIS Nyquist plots for g-C₃N₄-S, g-C₃N₄, BiOI, g-C₃N₄-S/BiOI, and g-C₃N₄/BiOI films. EIS data was obtained using AM1.5 G one sun illumination, in the frequency range of 0.1 to 10000 Hz, and at a potential of -0.2 V vs Ag/AgCl.

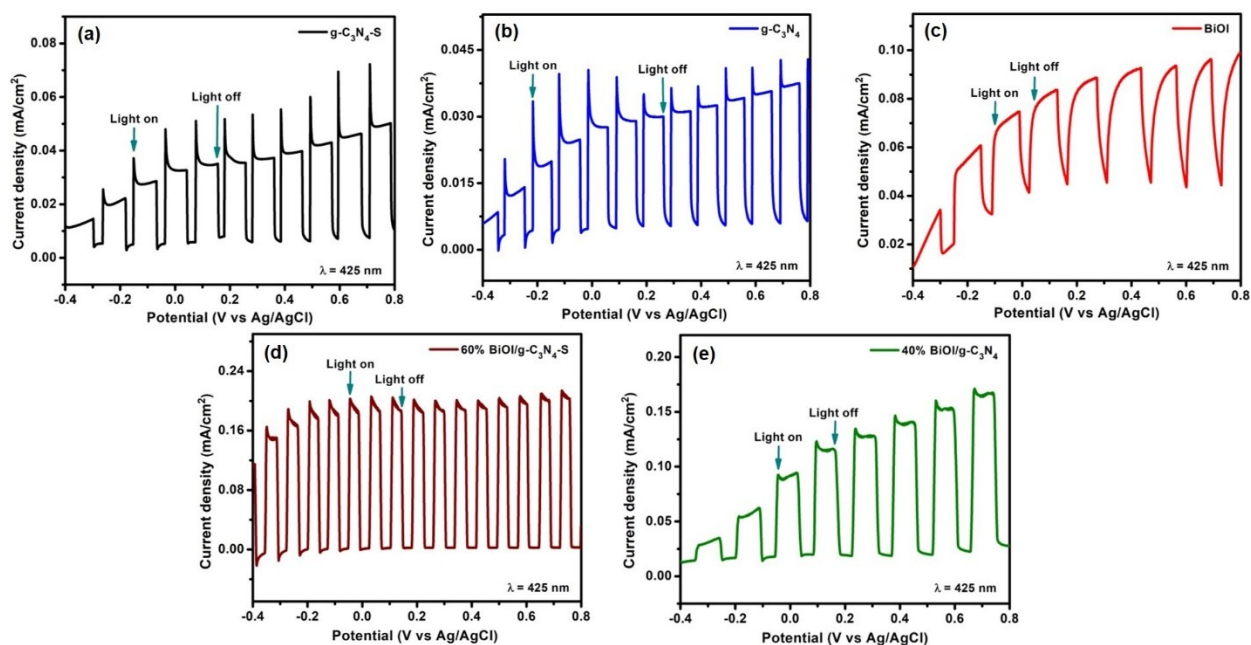


Figure S2. Photocurrent response under 425 nm LED light (54.15 W cm^{-2}) during on-off cycle for (a) g-C₃N₄-S (black), (b) g-C₃N₄ (blue), (c) BiOI (red), (d) g-C₃N₄-S/BiOI (wine red) and (e) g-C₃N₄/BiOI (green)

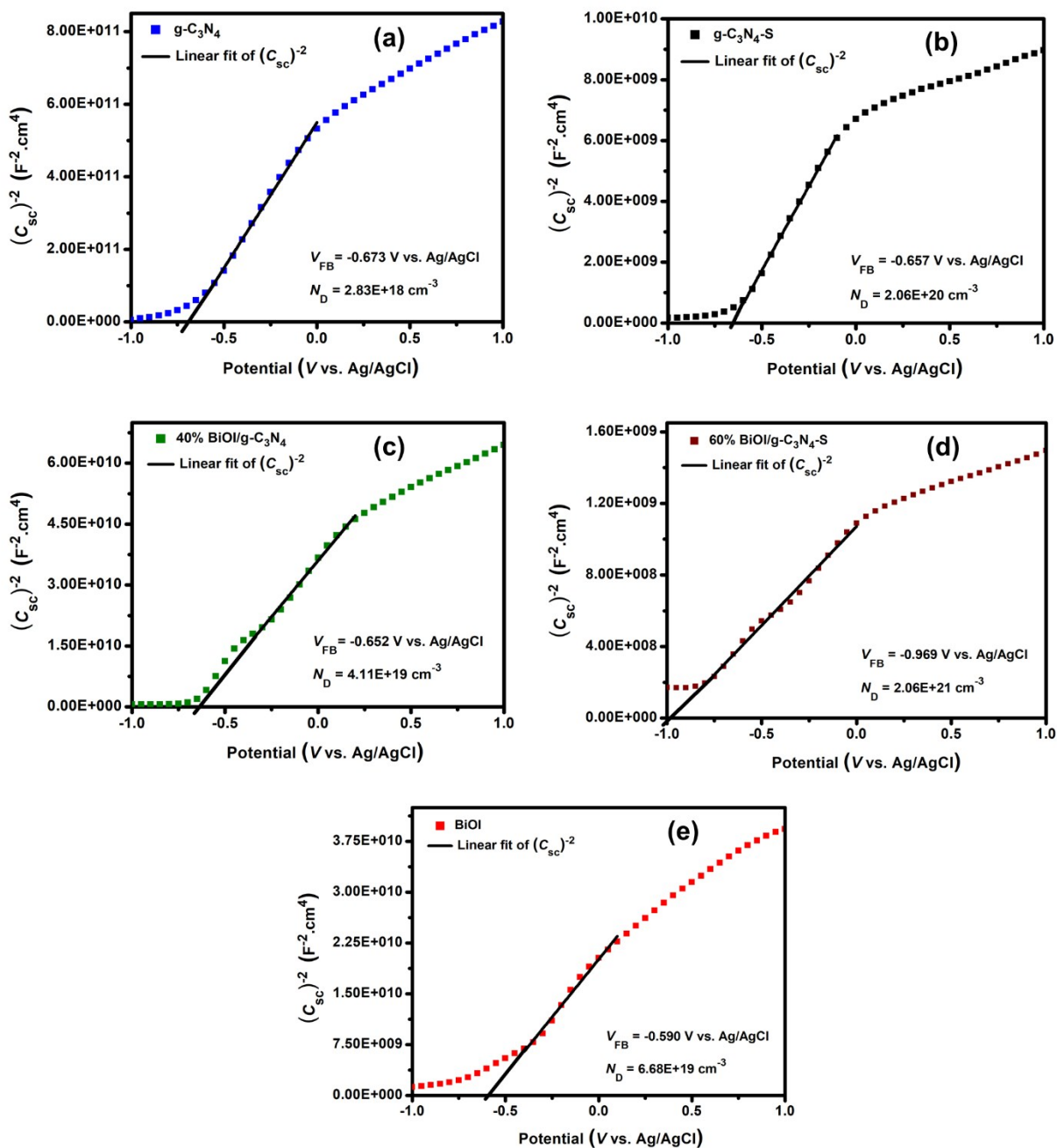


Figure S3. Mott-Schottky plots of bulk $g-C_3N_4$ (blue), $g-C_3N_4-S$ (black), 40% BiOI/ $g-C_3N_4$ (green), 60% BiOI/ $g-C_3N_4-S$ (wine red), and BiOI (red).

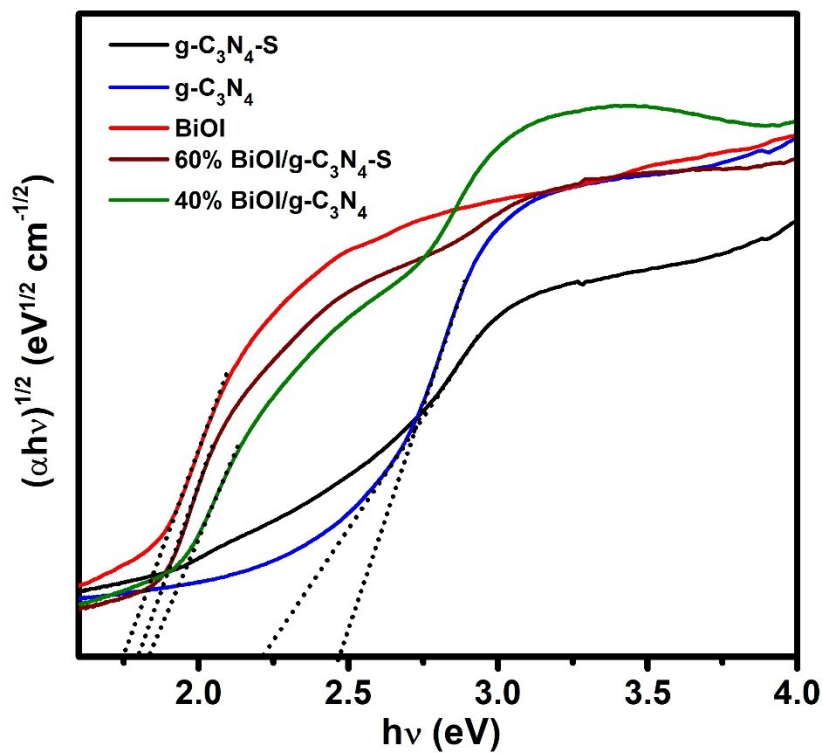


Figure S4. Tauc plots for the determination of the effective optical bandgaps of $\text{g-C}_3\text{N}_4\text{-S}$ (black), bulk $\text{g-C}_3\text{N}_4$ (blue), BiOI (red), $\text{g-C}_3\text{N}_4\text{-S/BiOI}$ (wine) and $\text{g-C}_3\text{N}_4\text{/BiOI}$ (olive green).

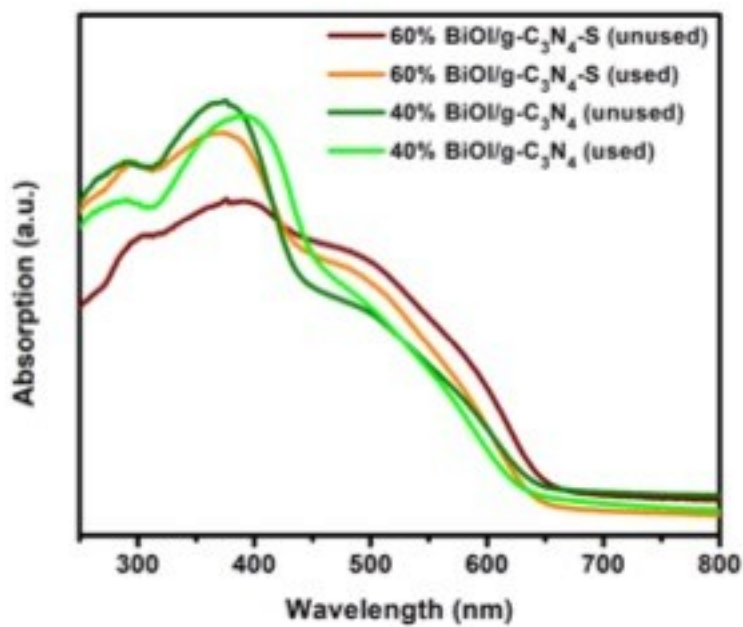


Figure S5. UV-Vis absorption spectra collected in diffuse reflectance mode (DR) mode for $g\text{-C}_3\text{N}_4\text{-S}/\text{BiOI}$ and $g\text{-C}_3\text{N}_4/\text{BiOI}$ heterostructures before (wine red and green) and after (orange and light green) several photoelectrochemical cycles respectively.

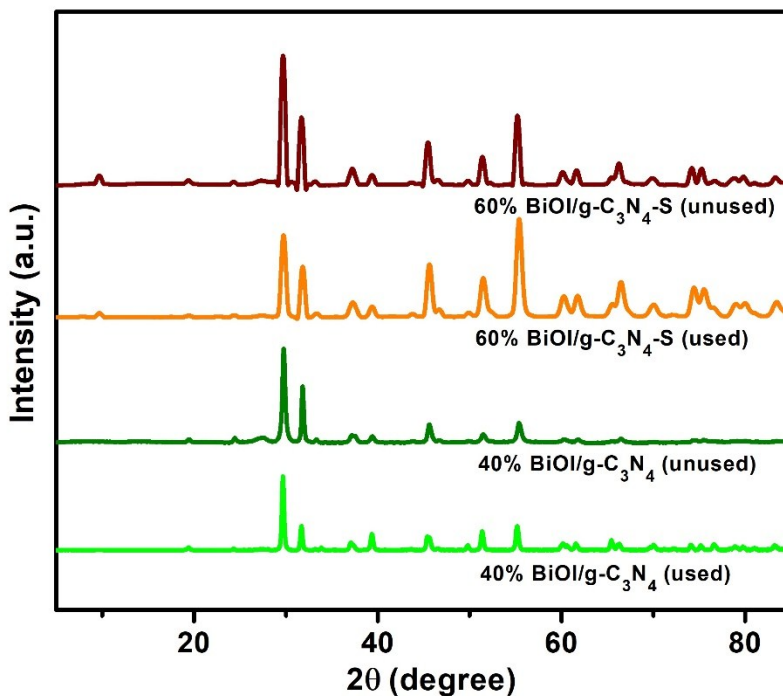


Figure S6. X-Ray diffractograms of $g\text{-C}_3\text{N}_4\text{-S}/\text{BiOI}$ and $g\text{-C}_3\text{N}_4/\text{BiOI}$ heterostructures before (wine red and green) and after (orange and light green) several photoelectrochemical cycles.

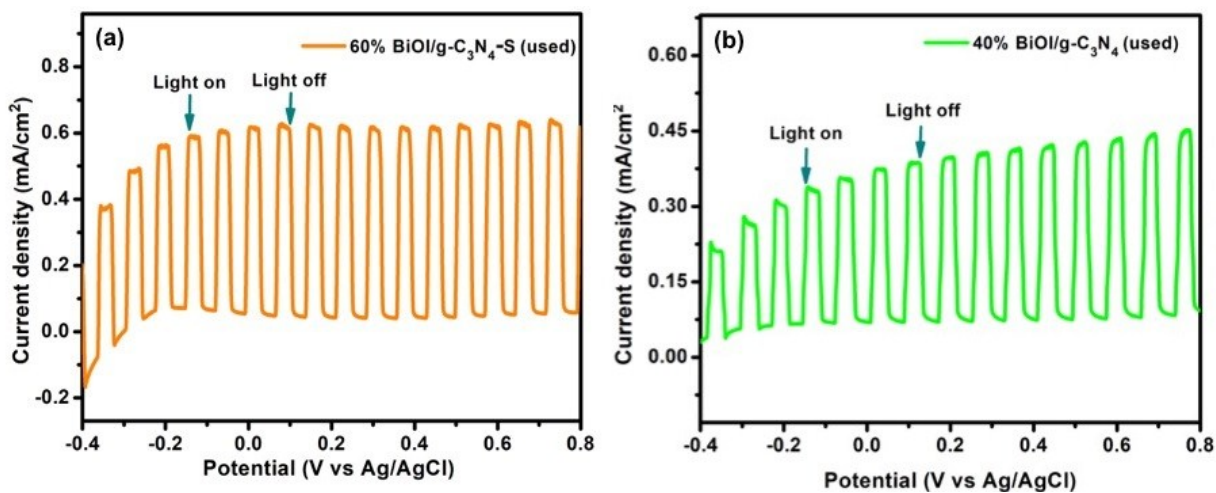


Figure S7. Photoelectrochemical re-use data for (a) $g\text{-C}_3\text{N}_4\text{-S}/\text{BiOI}$ (orange) and (b) $g\text{-C}_3\text{N}_4/\text{BiOI}$ (light green).

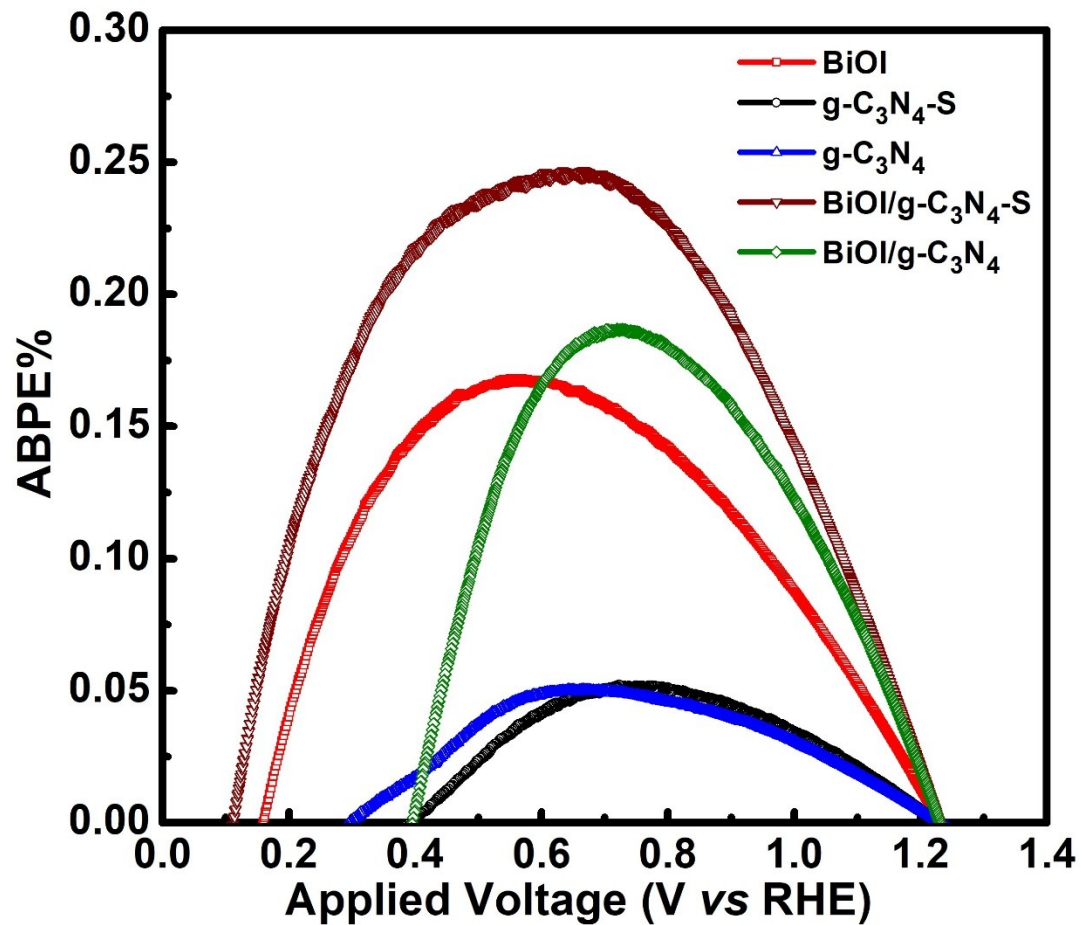


Figure S8. ABPE % vs RHE plot under AM1.5G light irradiation (100 mW cm^{-2}) for g-C₃N₄-S/BiOI (wine red), g-C₃N₄/BiOI (green), g-C₃N₄-S (black), g-C₃N₄ (blue), BiOI (g-C₃N₄-S).